PNAS RESEARCH ARTICLE | EARTH, ATMOSPHERIC, AND PLANETARY SCIENCES OPEN ACCESS

# Organic carbon concentrations in 3.5-billion-year-old lacustrine mudstones of Mars

Jennifer C. Stern[a,1], Charles A. Malespin[a], Jennifer L. Eigenbrode[a], Christopher R. Webster[b], Greg Flesch[b], Heather B. Franz[a], Heather V. Graham[a], Christopher H. House[c], Brad Sutter[d,e], Paul Douglas Archer Jr.[d,e], Amy E. Hofmann[b], Amy C. McAdam[a], Douglas W. Ming[e], Rafael Navarro-Gonzalez[f,2], Andrew Steele[g], Caroline Freissinet[h], and Paul R. Mahaffy[a]

Edited by Mark Thiemens, University of California, San Diego, La Jolla, CA; received January 28, 2022; accepted May 5, 2022

**The Sample Analysis at Mars instrument stepped combustion experiment on a Yellowknife Bay mudstone at Gale crater, Mars revealed the presence of organic carbon of Martian and meteoritic origins. The combustion experiment was designed to access refractory organic carbon in Mars surface sediments by heating samples in the presence of oxygen to combust carbon to $CO_2$. Four steps were performed, two at low temperatures (less than ∼550 °C) and two at high temperatures (up to ∼870 °C). More than 950 μg C/g was released at low temperatures (with an isotopic composition of $\delta^{13}C = +1.5 \pm 3.8$) representing a minimum of 431 μg C/g indigenous organic and inorganic Martian carbon components. Above 550 °C, 273 ± 30 μg C/g was evolved as $CO_2$ and CO (with estimated $\delta^{13}C = -32.9$ to $-10.1$ for organic carbon). The source of high temperature organic carbon cannot be definitively confirmed by isotopic composition, which is consistent with macromolecular organic carbon of igneous origin, meteoritic infall, or diagenetically altered biomass, or a combination of these. If from allochthonous deposition, organic carbon could have supported both prebiotic organic chemistry and heterotrophic metabolism at Gale crater, Mars, at ∼3.5 Ga.**

Mars | carbon isotopes | astrobiology

## Significance

This work presents the first quantification of bulk organic carbon in Mars surface sedimentary rocks, enabled by a stepped combustion experiment performed by the Curiosity Rover in Gale crater, Mars. The mudstone sample analyzed by Curiosity represents a previously habitable lacustrine environment and a depositional environment favorable for preservation of organics formed in situ and/or transported from a wide catchment area. Here we present the abundance of bulk organic carbon in these mudstone samples and discuss the contributions from various carbon reservoirs on Mars.

Understanding the inventory of carbon on Mars is relevant to the question of whether Mars was ever habitable. In addition, constraining the cycling of carbon between atmospheric and crustal reservoirs on past and present Mars is crucial to understanding Martian climate and surface environmental evolution. Meteorite analyses and in situ pyrolysis performed on Mars indicates that Mars regolith is a significant reservoir of carbon. While carbonate is the dominant carbon phase, geologically labile and refractory organic carbon is also present. A large body of carbon abundance and isotopic information exists for Mars meteorites (1–4), which predominantly represent igneous rocks excavated from the subsurface. Surface sedimentary rocks, however, can only currently be studied using in situ measurement techniques enabled by landers or rovers. Constraining the relative abundance of each carbon phase can increase our understanding of potential cycling of carbon between reservoirs during early Martian history.

The Sample Analysis at Mars (SAM) instrument suite on the Mars Science Laboratory (MSL) Curiosity Rover designed an experiment to combust refractory organic carbon to $CO_2$ to obtain its carbon isotopic composition ($\delta^{13}C$). This experiment was similar to laboratory stepped combustion of meteorites (2, 3, 5–7). SAM measured the abundances of evolved $CO_2$ and water as well as δD, $\delta^{13}C$, and $\delta^{18}O$ stable isotopic compositions for these volatiles. The δD results have been published elsewhere (8). Here we present carbon results of the combustion experiment, which represent the quantification of bulk refractory carbon in Mars surface materials.

## Cumberland Mudstone

The Curiosity landing site at the base of Aeolis Mons (Mount Sharp) at Gale crater (Fig. 1*A*) was chosen for ample orbital evidence of aqueous processes including layered phyllosilicate and sulfate deposits interpreted to represent global climate transitions on Mars (9). Crater count and stratigraphic relationships put the depositional timing of the lower layered sediments in Gale crater near the Hesperian-Noachian boundary (∼3.7 Ga), while the crater itself is Noachian in age (10, 11). Early in the mission, ∼444 m east of the Bradbury landing site, Curiosity encountered fine grain sedimentary rocks in the Sheepbed member of the Yellowknife Bay formation (Fig. 1*B*), interpreted to be a mudstone associated with a lacustrine setting (12). Two holes were drilled at the John Klein and Cumberland drill sites in the Sheepbed member (Fig. 1*C*). Drill fines of the Cumberland target (CB) were selected for combustion analysis.

Author contributions: J.C.S., C.A.M., and P.R.M. designed research with input from J.L.E., C.R.W., H.B.S., H.V.G., B.S., P.D.A., A.C.M., D.W.M., R.N.-G., C.F., and P.R.M.; J.C.S., C.A.M., J.L.E., C.R.W., G.F., H.B.F., H.V.G., B.S., P.D.A., A.C.M., D.V.M., R.N.-G., A.S., C.F., and P.R.M. performed research; J.C.S., C.R.W., G.F., and H.B.F. analyzed data; and J.C.S. wrote the paper with input from J.L.E., H.B.F., H.V.G., C.H.H., B.S., A.E.H., D.V.M., A.S., and P.R.M.

The authors declare no competing interest.

This article is a PNAS Direct Submission.



[1]To whom correspondence may be addressed. Email: Jennifer.C.Stern@nasa.gov.

[2]Deceased January 28, 2021

This article contains supporting information online at http://www.pnas.org/lookup/suppl/doi:10.1073/pnas.2201139119/-/DCSupplemental.

Published June 27, 2022.

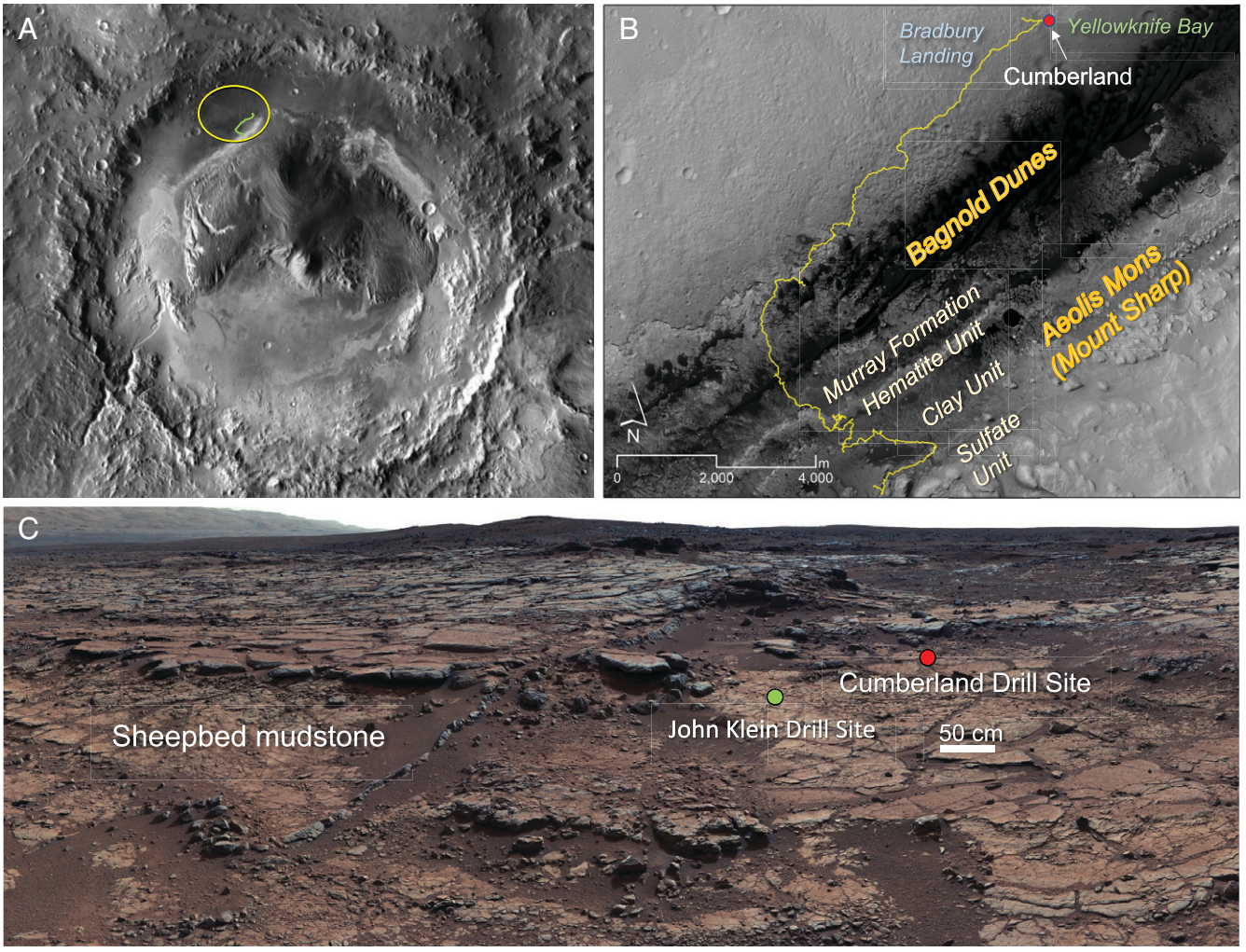


**Fig. 1.** (*A*) Landing ellipse of the Mars Science Laboratory Curiosity Rover at Gale Crater, Mars. (*B*) Rover Traverse from 2012 to 2022. Red dot shows the location of the Cumberland sample in the Yellowknife Bay formation. (*C*) Rover scale view of the Sheepbed mudstone member of the Yellowknife Bay formation, with locations of John Klein and Cumberland drill holes. Image Credit: NASA/JPL-Caltech/ASU, NASA/JPL-Caltech/Univ. of Arizona and Scott Rowland, NASA JPL-Caltech/MSSS.

The CB mudstone was extensively characterized by the MSL payload (13–15). Briefly, the Sheepbed member experienced at least two aqueous events post deposition with the nodules present being formed by trapped gases during early diagenesis. Fractures filled with Ca-sulfate indicated a subsequent aqueous event. Mineralogical analysis of the CB mudstone showed detrital basaltic minerals as well as Ca-sulfates, Fe-sulfides, and trioctahedral smectites (15, 16). The SAM instrument performed multiple evolved gas analysis (EGA) pyrolysis analyses on the CB mudstone, resulting in detection of chlorinated organics, hydroxyl water from smectite decomposition, low temperature $CO_2$ evolution, and high levels of oxychlorine and nitrate (17). The Yellowknife Bay formation was ultimately deemed to represent a potentially habitable shallow lacustrine environment based on evidence for circumneutral pH (15), high water activity/low salinity (14), variable redox states indicated by mineralogy and volatile content (15, 17), and presence of biologically relevant elements (13, 17), making it a target of interest for measuring bulk carbon abundance and carbon isotope composition.

## Methods

The SAM Combustion experiment used the SAM quadrupole mass spectrometer (QMS) and the SAM tunable laser spectrometer (TLS), which measures the abundance and isotopic composition of $CO_2$. Both instruments, as well as the entire SAM suite, have been described in detail elsewhere (18, 19). The SAM Combustion experiment differed significantly from SAM's nominal EGA pyrolysis experiment in which the QMS directly analyzed the gases released from samples heated to ~870 °C at 35 °C/min under He flow (18). Combustion was performed in a closed oven in the presence of oxygen, which was either sourced from oxychlorine in the sample or added to the cup as pure $O_2$ gas prior to the experiment using an onboard reservoir tank (18). Unlike pyrolysis, where gases evolved are continuously monitored using the QMS, gases produced during closed oven combustion were only released into the SAM manifold and analyzed by QMS and TLS upon completion of the heating step.

The combustion experiment was a four-step experiment performed in three separate experiment sequences executed on three sequential sols (*SI Appendix*, Table S1). The experiment was performed on a single aliquot of the CB mudstone sample, described above. The sample was heated to 550 °C or 870 °C and held at temperature for 25 min in a closed oven with either oxychlorine from the sample (step 1) or $O_2$ from the onboard tank (steps 2 to 4). Step 1 measured combusted $CO_2$ below 550 °C. After step 1, the sample cup was returned to the sample manipulation system (SMS) for exposure to instrument sources of carbon overnight to characterize background in step 2. Step 3 was performed at 870 °C and was designed to combust refractory carbon. Step 4 was also performed at 870 °C to combust remaining refractory carbon. Full experimental details are available in *SI Appendix*.

## Results

Abundance and isotope results are reported in Table 1. Error on TLS abundance and isotope values represent instrument precision. Error on QMS abundance values represents uncertainty associated

**Table 1. Selected TLS and QMS data for each step**

| | | Oxidant | TLS | | | | QMS | | | |
|---|---|---|---|---|---|---|---|---|---|---|
| | | $\delta^{18}O$ (‰) | $CO_2$ µmol | µg C/g | $CO_2$-$\delta^{13}C$ (‰) | $CO_2$-$\delta^{18}O$ (‰) | $CO_2$ µmol | CO nmol | $O_2$ nmol | $CH_4$ nmol |
| <550 °C | Step 1 | +41‰ Mars $O_2$ | 14 ± 0.1 | 957 ± 38 | +1.5 ± 3.8 | +55.0 ± 5.5 | NA | NA | NA | NA |
| | Step 2 | +20‰ Tank $O_2$ | 5.1 ± 0.03 | 340 ± 13 | −4.3 ± 4.3 | +58.2 ± 7.0 | 5.4 ± 0.3 | 72 ± 95 | 61 ± 19 | 182 ± 16* |
| <870 °C | Step 3 | +20‰ Tank $O_2$ | 2.5 ± 0.01 | 166 ± 7 | −16.2 ± 3.1 | +28 ± 5.6 | 3.0 ± 0.7 | 93 ± 206 | 180 ± 28 | 15 ± 4 |
| | Step 4 | +20‰ Tank $O_2$ | 1.2 ± 0.01 | 80 ± 3 | +2.5 ± 4.4 | +46 ± 4.5 | 1.0 ± 0.2 | 315 ± 49 | 24 ± 15 | 8 ± 1 |

Step 1 used oxychlorine native to Mars as the oxidant instead of tank $O_2$. No QMS data are available for step 1 due to QMS shut down. Steps 2 to 4 used the SAM $O_2$ tank carried for this purpose. The cup was returned to the sample manipulation system between steps 1 and 2 to estimate instrument background sources of carbon (*SI Appendix*). Step 3 was designed to access refractory carbon. Step 4 was designed to access refractory carbon not combusted in step 3

*$CH_4$ was saturated in step 2 so value represents lower limit.

with QMS calibration coefficients derived empirically during atmospheric runs on Mars during prelaunch calibration (*SI Appendix*, Table S2). QMS performance on Mars has been carefully monitored throughout the mission, and revisions to calibration coefficients are made routinely (20) to maintain accuracy. Additional uncertainty associated with the sample mass estimate is incorporated into calculations of µg C/g values presented in Table 2. Reported values represent lower end $CO_2$ abundance values, as several lines of evidence point to incomplete combustion, particularly in steps 2 to 4. While we do not have data for step 1, we predict that 24 to 30 µmol of $O_2$ was present based on SAM EGA pyrolysis data for CB (17), which should have been enough to overcome oxygen limitation. Steps 2 to 4, however, each had 3.7 µmol $O_2$. This amount was based on carbon abundance estimated using $CO_2$ measured during pyrolysis EGA of CB samples and the fact that resource limitations precluded adding large excesses of oxygen. We note that the molar ratio of carbon in $CO/CO_2$ was <3% except in step 4 where it was ∼30%, and $CH_4/CO_2$ was <1% except in step 2 where the QMS saturated on *m/z* 15, allowing us to only provide a lower limit value for methane. Because TLS precision is the same magnitude as uncertainties in the $\delta^{13}C$ of $CO_2$ associated with partial combustion reported in the literature (21), we do not add additional error to our isotope values.

$CO_2$ abundances measured by TLS and QMS (Table 1) for steps 2 to 4 allowed for cross-instrument validation of this data. The pressure of evolved volatiles in step 1 exceeded the safety limits set for the QMS, which shut itself down during analysis to prevent instrument damage. Therefore, a complete set of abundance data for steps 1 to 4 exists for TLS only, so all µg C/g data in the *Discussion* section was calculated using TLS values. TLS and QMS data were generally within error of one another for $CO_2$ abundances (Fig. 2). TLS combustion data for all steps combined yielded 23.2 ± 0.1 µmol $CO_2$ (0.5 ± 0.02 wt% $CO_2$) for this triple portion of sample. For comparison, average CB pyrolysis concentrations (single portion of 45 ± 18 mg) contained ∼2.0 to 3.1 µmol $CO_2$ (∼0.2 to 0.3 wt% $CO_2$) based on QMS data (17). Step 1 had the largest evolutions of $CO_2$. Step 3 evolved less $CO_2$ (2.5 to 3 µmol) than either step 1 or 2, and step 4 evolved the least $CO_2$ (1 µmol) of all steps.

**Table 2. Comparison of refractory carbon abundance in various planetary materials**

| Material | Carbon concentration (µg C/g) | Comment/Ref |
|---|---|---|
| Combustion $CO_2$ <550 °C Sheepbed mudstone, step 1 | 957 ± 38 | Combination of instrument C and at least ∼430 µg C/g Martian C |
| Combustion $CO_2$ <550 °C Sheepbed mudstone, step 2 | 340 ± 13 | Mostly instrument C |
| Combustion $CO_2$ + CO >550 °C Sheepbed mudstone, steps 3 and 4 | 273 ± 30 (201–273) | Refractory and mineral-stablized organic C, includes C from both $CO_2$ and CO. (Range reflects presence/absence of carbonate) |
| Pyrolysis <550 °C Sheepbed mudstone–$CO_2$ | 667–827 | Sutter et al. (23) |
| Pyrolysis >550 °C Sheepbed mudstone–$CO_2$ | 72 ± 7 | Sourced from carbonate, organics, or both |
| Estimated contribution from instrument sources to pyrolysis of CB mudstone | 163–237 | Calculated from MTBSTFA estimates from Freissinet et al. (24) |
| Pyrolysis >500 °C Sheepbed mudstone–hydrocarbon fragments | 5.6–6.7 | Eigenbrode et al. (26) |
| Pyrolysis >500 °C Murray mudstone–hydrocarbon fragments | 8.8–24.4 | Eigenbrode et al. (26) |
| Martian meteorite igneous organic carbon released by combustion >600 °C and <1,000 °C | 1.3–150 | Steele et al. (1); Grady et al. (2); Jull et al. (6, 7) |
| Estimates of total organic carbon concentration in Mars regolith due to exogenous inputs | 10<br>60<br>0.2–2.9 wt.% | Carrillo-Sanchez et al. (43)<br>Steininger et al. (42)<br>Schuerger et al. (41) |

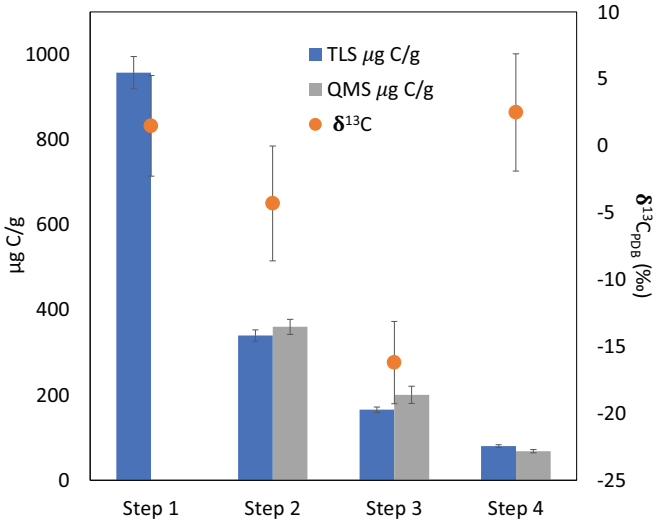


**Fig. 2.** TLS and QMS carbon abundances and TLS $\delta^{13}C$ data. Bulk $\delta^{13}C$ for steps 3 and 4 combined is $-3.6 \pm 3.1‰$.

TLS $\delta^{13}C$ and $\delta^{18}O$ values are reported with respect to terrestrial standards Vienna Pee Dee Belemnite (VPDB, referenced to National Bureau of Standards NBS 19) and Vienna Standard Mean Ocean Water (VSMOW), respectively (Table 1). Because $O_2$ from the oxygen tank was added in steps 2 to 4 for combustion, $\delta^{18}O$ values for $CO_2$ evolved in these steps was expected to be overprinted by the terrestrial tank value (~20‰). Step 1, however, used only Martian oxychlorine [$\delta^{18}O = 41 \pm 4‰$ (22)], as a source of oxygen.

Table 1 gives QMS abundance data for several additional species identified in combustion runs in steps 2 to 4 (additional QMS data in *SI Appendix*, Table S4). All carbon species other than $CO_2$ were present at nanomolar concentrations. CO was most abundant in step 4. $O_2$ was present in all steps at nanomolar abundance, although in step 3 all $O_2$ can be attributed to sulfate decomposition based on observed $SO_2$ abundance (see *SI Appendix*, Table S4), suggesting all added $O_2$ was utilized during this step. The $CO/CO_2$ ratio of 31% during step 4 is consistent with partial oxidation of a refractory phase. $CH_4$ was present in all steps and saturated the QMS in step 2.

## Discussion

**Low Temperature: Below 550 °C.** Over the entire temperature range of the experiment (~50° to 870 °C), the combustion run produced twice as much carbon in the form of $CO_2$ (1543 ± 41 μg C/g) as EGA pyrolysis runs (~667 to 827 μg C/g (23)) of the same CB mudstone. Low temperature (<550 °C) combustion (step 1) was responsible for most (957 ± 38 μg C/g) of this carbon.

Significant amounts of the carbon-bearing background contaminant, *N*-methyl-*N*-*tert*-butyldimethylsilyl-trifluoroacetamide (MTBSTFA) were present in both low temperature combustion steps due to elevated signals during prerun background scans for *m/z* 75, 127, and 147, diagnostic fragments derived from major byproducts of MTBSTFA reaction with water. Because the intent of step 2 was to characterize the amount of instrument carbon contributed by adsorption of MTBSTFA to the sample during overnight exposure in the SMS, MTBSTFA decomposition/combustion was expected the primary source of carbon in step 2. The amount of $CO_2$ produced during combustion step 2 (340 ± 13 μg C/g) was only slightly more than the 163 to 237 μg C/g calculated to be sourced from MTBSTFA during pyrolysis EGA runs of the same CB mudstone material (24). Interestingly, more MTBSTFA byproducts were present in step 1 background than in step 2 background, suggesting that a significant amount of the $CO_2$ evolved in step 1 was also due to combustion of MTBSTFA. However, it is notable that the 957 ± 38 μg C/g produced in step 1 represents at least 700 μg C/g in excess of calculated estimates for carbon (163-237 μg C/g) contributed by instrument sources during SAM EGA pyrolysis runs of CB (24). While this suggests a Martian source of low temperature carbon, we do not fully understand the long-term adsorption of MTBSTFA carbon to a sample while it sits in the SMS and cannot estimate instrument sources using concentration data alone.

Isotope ratios for low temperature steps are consistent with the presence of a $^{13}C$-enriched Martian end member (Fig. 3). If all the carbon detected during low temperature combustion in steps 1 and 2 was derived from MTBSTFA, then $\delta^{13}C$ of $CO_2$ in both low temperature steps would reflect this instrument source of carbon at $\delta^{13}C = -35‰$. Our step 1 and 2 combustion $\delta^{13}C$ values were $+1.5 \pm 3.1‰$ and $-4.3 \pm 4.3‰$, respectively, and fall within the range of $\delta^{13}C$ values calculated for the $CO_2$ peak evolved between 180 to 450 °C in SAM EGA pyrolysis of CB samples, which show a weighted average $\delta^{13}C$ of $-6 \pm 11‰$ (22). While a mass balance approach involves too many assumptions to isolate individual contributions from different carbon sources, these $\delta^{13}C$ values can put constraints on the maximum worst case contribution of MTBSTFA to the sample in step 1. Assuming a two-end member mixing model with a $^{13}C$ depleted end member (MTBSTFA at $\delta^{13}C = -35‰$) and a $^{13}C$-enriched end member (carbonate at $\delta^{13}C = +45‰$), a maximum of 55% of the carbon could derive from MTBSTFA decomposition in step 1 (detailed calculation in S9). This leaves a minimum of 45%, or 431 μg C/g, of carbon derived from indigenous Martian or exogenous carbon. Interpretation of step 2 isotope data are complicated by the addition of instrument background carbon prior to combustion when the sample was returned to the SMS, coupled with the fact that any partial combustion in step 1 (while not expected) would have resulted in $^{13}C$ enrichment of any step 1 residual carbon through Rayleigh distillation.

The source of the ≥431 μg C/g non-instrument carbon could derive from a range of $^{13}C$ enriched Martian and exogenous (meteoritic) reservoirs (Fig. 3). SAM EGA pyrolysis experiments of 13 samples demonstrated that $CO_2$ evolved below 550 °C had a broad range of $\delta^{13}C$ ($-25 \pm 20‰$ to $+56 \pm 11‰$) representing multiple carbon sources (22). In addition to the previously discussed instrument carbon source, carbon could come from oxidation or decarboxylation of Martian organics or exogenous carbon (17, 22–28). Recent work (28) showed that SAM-like pyrolysis of metastable organic salts such as acetates and oxalates produce $CO_2$ and CO below 550 °C, putting upper limits for abundances of these compounds in SAM pyrolysis experiments as high as 2 to 3 wt%. These molecules may be present as radiolytic decomposition products of more complex organics (29, 30) or could represent simple molecules formed in situ by photolysis or electrochemistry (4, 22). Depending on formation mechanism, these molecules would likely be 10 to 30‰ depleted in $^{13}C$ with respect to the Martian atmosphere at the time of their formation (22, 31), resulting in $\delta^{13}C$ values of ~+15 to 35‰ for photochemically created molecules in the current atmosphere. Carbonate decrepitation occurs over a broad temperature range (400° to 700 °C) in stepped combustion of meteorites (2). Carbonates in Noachian aged ALH84001 evolved $CO_2$ with $\delta^{13}C$ values of +32.5

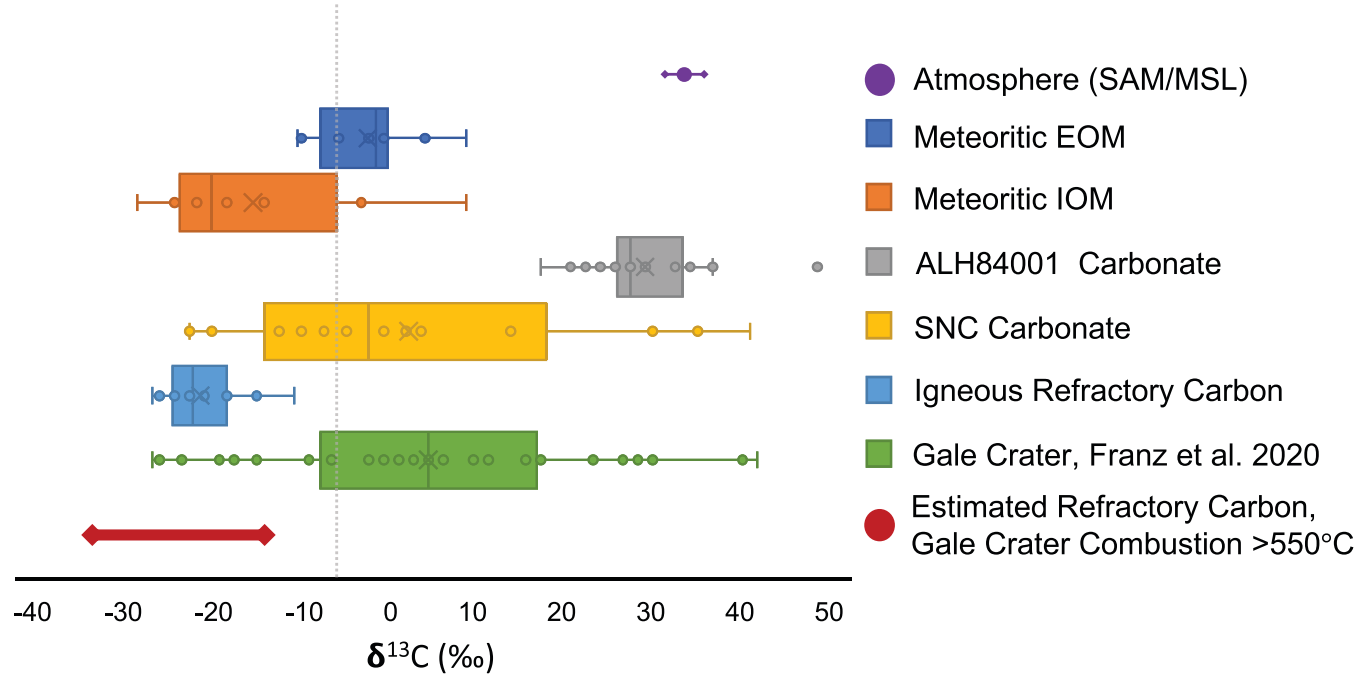


**Fig. 3.** Carbon isotopic composition of carbon reservoirs on Mars. Our combustion data overlap with both igneous refractory carbon, meteoritic organics, and carbonate carbon. Atmospheric data from (29); Meteoritic EOM from (25, 26); Meteoritic IOM data from (34); Carbonate SNC range from (48); ALH84001 data from (7, 50); Igneous refractory carbon from (1); Gale Crater data from (13) Box and whiskers show the median, upper and lower quartiles, and maximum and minimum values, with outlier values shown as black dots.

to 40‰ between 430 and 600 °C in stepped combustion experiments (7). Although CheMin XRD did not identify carbonate above the 1% detection limit, the large amount of amorphous material detected by CheMin may indicate the presence of microcrystalline carbonate, which can evolve $CO_2$ <550 °C. In addition, HCl evolved from oxychlorine decomposition can also drive $CO_2$ evolution temperatures below 550 °C (17, 23). Finally, solvent extractable organic matter (EOM) in meteorites represents a less $^{13}C$ enriched reservoir of carbon than carbonates or modern photochemical or electrochemical carbon, with values generally averaging around $\delta^{13}C = +5‰$ (32).

Oxygen isotopic compositions of $CO_2$ evolved below 550 °C suggest contributions from an isotopically enriched component in the sample. The $\delta^{18}O$ weighted average of $O_2$ evolved from sand sample Rocknest and CB was ~40‰ (22), which reflects the Martian oxychlorine source. $\delta^{18}O$ of $CO_2$ in step 1 was +55 ± 5.5‰, more enriched than oxychlorine and similar to atmospheric $CO_2$ ($\delta^{18}O = +50‰$ (33)). Early thermal decomposition of siderite could also produce $^{18}O$ enriched $CO_2$; siderite precipitated at 25 °C would be $^{18}O$ enriched by about 10‰ with respect to modern atmospheric $CO_2$. In steps 2 to 4, $\delta^{18}O$ of $CO_2$ produced by combustion should have been approximately +20‰ (SAM tank value). Step 2 $\delta^{18}O$ values were very similar to step 1, suggesting the addition of $^{18}O$ enriched $O_2$ to tank $O_2$, along with the fact that the $CO_2$ abundance in step 2 (5.41 μmol) was larger than the moles of $O_2$ added (3.7 μmol). Based on mass balance calculations, the $\delta^{18}O$ value measured in step 2 would require contribution from an $O_2$ source with $\delta^{18}O$ greater than +100‰, suggesting that instead isotopic exchange of $CO_2$ with isotopically enriched $O_2$ reservoirs in mudstone (e.g., silicates or oxides) may have occurred during the analysis.

**High temperature: 550° to 870 °C.** More carbon was evolved as $CO_2$ between 550° and 870 °C during the closed oven SAM combustion experiment than by SAM EGA pyrolysis alone. This additional $CO_2$ is likely from combustion of a broad suite of refractory organic components in the sample. High temperature combustion (steps 3 and 4) yielded a total of 246 ± 7 μg C/g as $CO_2$. In step 3 combustion appears to be nearly complete, with $CO/CO_2$ ~3% and $CH_4/CO_2$ < 1%. However, in step 4, 21 μg C/g was present as CO ($CO/CO_2 = 31\%$), suggesting that step 4 combustion did not go to completion. Adding CO carbon from steps 3 and 4 to $CO_2$ carbon yields a total high-temperature carbon abundance of 273 ± 32 μg C/g (Table 2).

Some portion of this carbon may be from thermal decomposition of carbonate. Above 550 °C, EGA pyrolysis of triple-portion CB mudstone aliquots resulted in an average concentration of 72 ± 7 μg C/g based on $CO_2$ QMS data. This release occurred at temperatures near those expected for calcite decrepitation (~700 to 750 °C). However, $CO_2$ coevolved with CO and *m/z* associated with decomposition of sulfates, which have been identified in this sample (17). These factors support either release of mineral-bound organic matter during sulfate decomposition or organic oxidation by $O_2$ sourced from the decomposition of sulfates. In addition, Eigenbrode et al. (26) found organic carbon evolving from the same sample material at these temperatures, described below. Therefore, we report a range of 201 to 273 μg C/g for refractory organic carbon, as we cannot further constrain the carbonate abundance in the sample.

Eigenbrode, et al. (26) showed that masses consistent with aliphatic, aromatic, and organic-sulfur compounds were present above background at temperatures above 500 °C in samples of the same Yellowknife Bay mudstone. Total carbon concentration for these detected compounds was ~40× less than that detected by high-temperature combustion (Table 2). The differences between carbon concentrations detected by combustion and pyrolysis are due to the nature of the experiments. At high temperatures above 500° to 550 °C, pyrolysis is limited to thermal cleavage or decarboxylation of macromolecules or mineral decrepitation/decomposition with subsequent release of

compounds. As such, a significant fraction of more thermally recalcitrant organic matter is expected to be left undetected in the sample. In contrast, combustion leverages both thermal and oxidative processing of organic components including the most refractory macromolecular material, thus releasing more carbon detected as a single gas, $CO_2$. Assuming the ratio of high-temperature combustion carbon to pyrolysis organic carbon for CB reported by Eigenbrode et al. (26), Murray mudstone could have refractory organic carbon concentrations up to 730 μg C/g, depending on carbonate abundance (see *SI Appendix*, Table S7).

High-temperature $CO_2$ should represent carbon in the sample and not instrument background. SAM pyrolysis and laboratory testing have demonstrated that MTBSTFA decomposition occurs mostly below 550 °C, particularly in the presence of strong oxidants (see *SI Appendix*, Figs. S1 and S2). However, as previously mentioned, there is evidence for partial combustion in some steps. Because the combustion experiment was performed in a closed oven at 550 °C for 25 min in the presence of soil oxidants (step 1) and added $O_2$ (step 2), most volatile compounds were likely released in these first two low-temperature steps by thermal desorption, oxidation, and some pyrolytic cleavage from macromolecules and organic mineral-bound or mineral-enclosed components. Upon oxidation at 870 °C, more thermal energy was available to break the stronger molecular bonds persisting in macromolecules and decomposed minerals that may be trapping organic components. Therefore, $CO_2$ evolved at high temperatures reflects a more refractory carbon pool within this sample that is likely to include macromolecules and organic mineral-bound/enclosed components. This is consistent with the reported detections of complex organics evolved during high-temperature SAM pyrolysis (26).

The $^{13}C$ enrichment in step 4 ($\delta^{13}C = +2.5 \pm 4.4‰$) compared to step 3 ($\delta^{13}C = -16.2 \pm 3.1‰$) may represent a more refractory reservoir of carbon that was released during the second heating step above 550 °C. Rayleigh type isotopic distillation may have resulted in the $^{13}C$ enrichment of the remaining recalcitrant carbon in step 4. Alternatively, the difference in $\delta^{13}C$ values between steps 3 and 4 may be due to isotopic heterogeneity. These values overlap with multiple carbon sources (Fig. 3) including carbonate (5, 34, 35), meteoritic insoluble organic matter (IOM) (36), and magmatic carbon (1), and likely represent a mixture of these carbon reservoirs. By mass balance, a bulk $\delta^{13}C$ value for total carbon released in steps 3 + 4 is $\delta^{13}C = -10.1‰$. While we cannot constrain the amounts and isotopic compositions of every component of this mixture, a two end-member mixing model can help bound the isotopic composition of the organic carbon considering the case where no carbonate is present and the case where all 72 μg C/g $CO_2$ detected in SAM EGA pyrolysis was from calcite of $\delta^{13}C = +45‰$. Such a calculation produces a range of $\delta^{13}C$ values from −10.1‰ to −32.9‰, depending on how much carbonate is in the sample. Based on the behavior of both CO and $SO_2$ in the sample, which support the present of some amount of organic material, it is likely that the value is somewhere in the middle. This is broadly consistent with refractory or macromolecular carbon (1, 2) but does not preclude contributions from other carbon sources.

With regards to $\delta^{18}O$ composition, steps 3 ($\delta^{18}O = +28 \pm 5.6‰$) and 4 ($\delta^{18}O = +46 \pm 4.5‰$) showed enrichment in $^{18}O$ with respect to the SAM tank value of $\delta^{18}O = 20‰$, suggesting the addition of $O_2$ from a source in equilibrium with or enriched with respect to Martian atmosphere ($\delta^{18}O = +50‰$ (33)). To achieve the measured value in step 3, about one-third of the oxygen would have had to come from carbonate, theoretically possible if all $CO_2$ detected in pyrolysis experiments was from carbonate. However, to achieve the heavier step 4 values, 75 to 90% of the oxygen in $CO_2$ would have to come from carbonate, which is inconsistent with pyrolysis experiments. This suggests exchange with silicate oxygen or structural water, which is highly likely at these temperatures.

The source of the organic carbon evolving high-temperature $CO_2$ during combustion is not easily resolved. Our $\delta^{13}C$ values for combusted $CO_2$ ($\delta^{13}C = -10.1‰$ to $-32.9‰$) do not show the same extreme $^{13}C$ depletions as recently reported $\delta^{13}C$ values for $CH_4$ evolved during SAM EGA pyrolysis experiments (−96‰ to −71‰) on the same CB samples (37). This is likely because $\delta^{13}C$ of combusted $CO_2$ is a bulk measurement of all carbon in the sample, and $CH_4$ only represents a very small portion (~0.2‰) of the total carbon in the sample. Potential sources of refractory carbon include exogenous organic matter from meteoritic infall, geologic carbon produced by abiotic processes, geologically reworked biological organics, or a combination of these. Here we consider each possible source.

High-temperature combustion $CO_2$ ($\delta^{13}C = -10.1‰$ to $-32.9‰$) has similar values to insoluble organic carbon evolved from meteorites (Fig. 3). Pyrolysis data for the isotopic composition of organic carbon evolved above 800 °C from carbonaceous meteorites gives values of around −16 to −1 ‰ (38). The range for IOM in meteorites is broader, with $\delta^{13}C = -20$ to −5‰ (32, 39). Mars surface sedimentary composition is greatly influenced by influx of meteoritic material (40) and the similarity between the distribution of organics found in the Murchison and Nahkla meteorites suggests that Mars meteorites contain a component of this exogenous carbon (1, 39). Concentration of total impact deposited organic carbon in Mars regolith is highly dependent on model assumptions such as influx, impact gardening depth, and total organic carbon content of exogenous materials, but estimates range anywhere from 10 μg C/g up to 2.9 wt.% C (41–43). It is therefore likely that the Sheepbed mudstone forming in the Yellowknife Bay Lake catchment would have been predisposed to accumulate exogenous carbon. However, studies predict that high rates of radiolytic destruction of light organics in Mars surface environments would outpace exogenous influx (44–46) and result in far lower concentrations of organics in the near surface. The abundance of exogenous organic carbon incorporated into the sediments lithified to form the Sheepbed mudstone would be determined by factors such as sedimentation rates and geochemical environment. The young surface exposure age dates for the Sheepbed mudstone (78 ± 30 Ma (47)), likely resulting from early burial and recent scarp retreat, suggest that irradiation and consequent destruction of organics in Sheepbed mudstone may have been limited compared to other Martian surfaces with older exposure ages. This supports the inclusion of meteoritic organics in the CB mudstone.

$CO_2$ evolved during stepped combustion of many Mars meteorites above 600 °C is associated with igneous refractory carbon (2). Igneous Mars rocks contain 18 ± 26 ppm of refractory organic carbon synthesized in-situ, with an average $\delta^{13}C$ of $-19.1 \pm 4.5‰$ (1), also within the range of $\delta^{13}C$ reported for combustion of CB sediments in step 3. However, the combustion values need to be considered in the context of the CB sample as a lacustrine mudstone, which has likely seen a different geological history than the deeply excavated igneous rocks that comprise most of the Martian meteorites reported to date. The only Mars meteorite sampling Martian surface breccia is NWA 7034, which gave organic carbon abundance of 22 ± 10 μg/g with $\delta^{13}C$ of $-23.4 \pm 0.73‰$, similar to the average for shergottites (48). Therefore, it is likely that some component of the total organics evolving $CO_2$ in combustion of CB sample includes the

refractory organic carbon component associated with basaltic minerals seen in Mars meteorites deposited as transported detritus to the Yellowknife Bay Lake and preserved in Sheepbed mudstone.

The $\delta^{13}C$ of carbon evolved as $CO_2$ at 870 °C in SAM combustion neither rules out nor confirms geological processing of biological organics, which could have been produced or deposited in lake sediments and converted to kerogen preserved in mudstones by exposure to heat from regional hydrothermal activity during burial (49) and sulfurization (26). Biological carbon fixation on Earth has a broad range of fractionations, with $^{13}C$ depletion ranging from a few per mil to tens of per mil with respect to carbon source, depending on metabolism and organism. This, coupled with the wide range of isotopic compositions in carbon reservoirs on Mars (Fig. 3), complicates the use of isotopes to confirm or eliminate the potential for biological carbon fixation processes on Mars. Therefore, combustion $\delta^{13}C$ isotopes cannot be used to support a biological origin for refractory carbon, but do not rule out this possible source.

Recent reports of a diverse array of organics released by SAM EGA pyrolysis at these temperatures in other Sheepbed mudstone samples, including sulfurized organics (26), highlight the preservation potential of these sediments. The mineralogy of the CB sample would have likewise supported preservation of organics through binding to phyllosilicates and Al-Fe oxyhydroxides, as well as iron sulfides, which could have provided a sink for oxygen during diagenesis (26). However, without additional isotopic or compositional data on these or other sources, it is difficult to further constrain the possibilities.

## Conclusions

The SAM combustion experiment results support the presence of Martian carbon combusted or thermally evolved below and above 550 °C. The carbon isotopic composition of low-temperature $CO_2$ is consistent with the presence of a $^{13}C$-enriched carbon phase of Martian origin in addition to carbon contributions from instrument background (MTBSTFA). Instrument background contributed a maximum of 55% of the total carbon detected in step 1. The remaining 431 μg C/g carbon could come from organics created by photochemistry, meteoritic organics, carbonate, or a mixture of these.

More $CO_2$ was evolved above 550 °C in closed-oven combustion experiments than in previous pyrolysis experiments on the same sample, indicating that combustion released more mineral-bound and refractory carbon than pyrolysis of the same materials. The combustion experiment results above 550 °C revealed that 201 to 273 μg C/g of organic carbon was preserved in the 3.5-billion-year-old Yellowknife Bay lacustrine mudstones, roughly 40 times more organic carbon than previously reported by Eigenbrode et al. (26), and more organic carbon than reported for Martian meteorites (1). Isotopic compositions of this high-temperature organic carbon are consistent with the same igneous refractory or macromolecular carbon phase detected in Mars meteorites with contributions from meteoritic organics, but a biological origin for some amount of carbon cannot be ruled out.

Assuming a similar ratio of organic carbon released during combustion to pyrolysis organic carbon as seen in Yellowknife Bay samples, estimated organic carbon concentrations for the Murray mudstone could approach 800 μg C/g, depending on the amount of carbonate present. While results suggest this carbon was largely refractory or mineral-bound in nature, which attests to its preservation over billions of years, it remains to be determined if there is chemical information preserved within it that pinpoint how it was formed and what processing may have altered it since deposition.

**Data Availability.** Flight mass spectrometry and tunable laser spectrometry data have been deposited in the Geosciences Node of NASA's Planetary Data System (https://pds-geosciences.wustl.edu/missions/msl/sam.htm). All study data are included in the article and/or *SI Appendix*.

**ACKNOWLEDGMENTS.** We thank the NASA Mars Exploration Program for support of the MSL project. We acknowledge the hard work and dedication of the Mars Science Laboratory Engineering, Operations, and Science Teams who made this research possible. In addition, we acknowledge the SAM instrument Engineering, Operations, and Science teams, for their support in development of the combustion experiment and for productive discussions of results. We thank Scott Rowland for the map of the MSL traverse to date in Fig. 1. We also thank Paul Niles for helpful discussions and additional insights, as well as Alex Sessions and two anonymous reviewers for their suggestions and insights.

Author affiliations: [a]Solar System Exploration Division, NASA Goddard Space Flight Center, Greenbelt, MD 20771; [b]NASA Jet Propulsion Laboratory, California Institute of Technology, Pasadena, CA 91109; [c]Department of Geosciences, The Pennsylvania State University, University Park, PA 16802; [d]Jacobs Technology, Houston, TX 77058; [e]NASA Johnson Space Center, Houston, TX 77058; [f]Instituto de Ciencias Nucleares, Universidad Nacional Autónoma de México, Mexico City, 04510, Mexico; [g]Geophysical Laboratory, Carnegie Institution of Washington, Washington, DC 20015; and [h]Laboratoire Atmosphères, Observations Spatiales - Institut Pierre-Simon Laplace (LATMOS-IPSL), CNRS-Guyancourt, 78280 Guyancourt, France

1. A. Steele, F. M. McCubbin, M. D. Fries, The provenance, formation, and implications of reduced carbon phases in Martian meteorites. *Meteorit. Planet. Sci.* **51**, 2203–2225 (2016).
2. M. Grady, A. Verchovsky, I. Wright, Magmatic carbon in Martian meteorites: Attempts to constrain the carbon cycle on Mars. *Int. J. Astrobiol.* **3**, 117–124 (2004).
3. A. Steele *et al.*, A reduced organic carbon component in Martian basalts. *Science* **337**, 212–215 (2012).
4. A. Steele *et al.*, Organic synthesis on Mars by electrochemical reduction of $CO_2$. *Sci. Adv.* **4**, eaat5118 (2018).
5. I. Wright, M. M. Grady, C. Pillinger, Chassigny and the nakhlites: Carbon-bearing components and their relationship to Martian environmental conditions. *Geochim. Cosmochim. Acta* **56**, 817–826 (1992).
6. A. J. Jull, J. W. Beck, G. Burr, Isotopic evidence for extraterrestrial organic material in the Martian meteorite, Nakhla. *Geochim. Cosmochim. Acta* **64**, 3763–3772 (2000).
7. A. J. T. Jull, C. Courtney, D. A. Jeffrey, J. W. Beck, Isotopic evidence for a terrestrial source of organic compounds found in Martian meteorites Allan Hills 84001 and Elephant Moraine 79001. *Science* **279**, 366–369 (1998).
8. P. R. Mahaffy *et al.*; MSL Science Team, Mars atmosphere. The imprint of atmospheric evolution in the D/H of Hesperian clay minerals on Mars. *Science* **347**, 412–414 (2015).
9. R. Milliken, J. Grotzinger, B. Thomson, Paleoclimate of Mars as captured by the stratigraphic record in Gale Crater. *Geophys. Res. Lett.* **37**, L04201 (2010).
10. L. L. Deit, E. Hauber, F. Fueten, M. Pondrelli, A. P. Rossi, R. Jaumann, Sequence of infilling events in Gale Crater, Mars: Results from morphology, stratigraphy, and mineralogy. *J. Geophys. Res. Planets* **118**, 2439–2473 (2013).
11. B. Thomson *et al.*, Constraints on the origin and evolution of the layered mound in Gale Crater, Mars using Mars Reconnaissance Orbiter data. *Icarus* **214**, 413–432 (2011).
12. J. P. Grotzinger *et al.*, Mars science laboratory mission and science investigation. *Space Sci. Rev.* **170**, 5–56 (2012).
13. J. P. Grotzinger *et al.*; MSL Science Team, A habitable fluvio-lacustrine environment at Yellowknife Bay, Gale crater, Mars. *Science* **343**, 1242777 (2014).
14. S. M. McLennan *et al.*; MSL Science Team, Elemental geochemistry of sedimentary rocks at Yellowknife Bay, Gale crater, Mars. *Science* **343**, 1244734 (2014).
15. D. T. Vaniman *et al.*; MSL Science Team, Mineralogy of a mudstone at Yellowknife Bay, Gale crater, Mars. *Science* **343**, 1243480 (2014).
16. T. F. Bristow *et al.*, The origin and implications of clay minerals from Yellowknife Bay, Gale crater, Mars. *Am. Mineral.* **100**, 824–836 (2015).
17. D. W. Ming *et al.*; MSL Science Team, Volatile and organic compositions of sedimentary rocks in Yellowknife Bay, Gale crater, Mars. *Science* **343**, 1245267 (2014).
18. P. R. Mahaffy *et al.*, The sample analysis at Mars investigation and instrument suite. *Space Sci. Rev.* **170**, 401–478 (2012).
19. C. R. Webster, P. R. Mahaffy, Determining the local abundance of Martian methane and its' $^{13}C/^{12}C$ and D/H isotopic ratios for comparison with related gas and soil analysis on the 2011 Mars Science Laboratory (MSL) mission. *Planet. Space Sci.* **59**, 271–283 (2011).
20. H. B. Franz *et al.*, Reevaluated Martian atmospheric mixing ratios from the mass spectrometer on the Curiosity rover. *Planet. Space Sci.* **109-110**, 154–158 (2015).
21. P. D. Warwick, L. F. Ruppert, Carbon and oxygen isotopic composition of coal and carbon dioxide derived from laboratory coal combustion: A preliminary study. *Int. J. Coal Geol.* **166**, 128–135 (2016).
22. H. B. Franz *et al.*, Indigenous and exogenous organics and surface–atmosphere cycling inferred from carbon and oxygen isotopes at Gale crater. *Nat. Astron.* **4**, 526–532 (2020).
23. B. Sutter *et al.*, Evolved gas analyses of sedimentary rocks and eolian sediment in Gale Crater, Mars: Results of the curiosity Rover's sample analysis at Mars (SAM) instrument from Yellowknife Bay to the Namib Dune. *J. Geophys. Res. Planets* **122**, 2574–2609 (2017).
24. C. Freissinet *et al.*, Organic molecules in the Sheepbed Mudstone, Gale Crater, Mars. *J. Geophys. Res. Planets* **120**, 495–514 (2015).

25. P. D. Archer *et al.*, Abundances and implications of volatile-bearing species from evolved gas analysis of the Rocknest aeolian deposit, Gale Crater, Mars. *J. Geophys. Res. Planets* **119**, 237–254 (2014).
26. J. L. Eigenbrode *et al.*, Organic matter preserved in 3-billion-year-old mudstones at Gale crater, Mars. *Science* **360**, 1096–1101 (2018).
27. L. A. Leshin *et al.*; MSL Science Team, Volatile, isotope, and organic analysis of martian fines with the Mars Curiosity rover. *Science* **341**, 1238937 (2013).
28. J. M. T. Lewis *et al.*, Pyrolysis of oxalate, acetate, and perchlorate mixtures and the implications for organic salts on Mars. *J. Geophys. Res. Planets* **126**, e2020JE006803 (2021).
29. S. A. Benner, K. G. Devine, L. N. Matveeva, D. H. Powell, The missing organic molecules on Mars. *Proc. Natl. Acad. Sci. U.S.A.* **97**, 2425–2430 (2000).
30. A. C. Fox, J. L. Eigenbrode, K. H. Freeman, Radiolysis of macromolecular organic material in Mars-relevant mineral matrices. *J. Geophys. Res. Planets* **124**, 3257–3266 (2019).
31. J. Davidson *et al.*, Carbon kinetic isotope effect in the reaction of CH4 with HO. *J. Geophys. Res. D Atmospheres* **92**, 2195–2199 (1987).
32. M. A. Sephton, Organic compounds in carbonaceous meteorites. *Nat. Prod. Rep.* **19**, 292–311 (2002).
33. C. R. Webster *et al.*; MSL Science Team, Isotope ratios of H, C, and O in $CO_2$ and $H_2O$ of the Martian atmosphere. *Science* **341**, 260–263 (2013).
34. P. B. Niles, W. V. Boynton, J. H. Hoffman, D. W. Ming, D. Hamara, Stable isotope measurements of martian atmospheric $CO_2$ at the Phoenix landing site. *Science* **329**, 1334–1337 (2010).
35. I. Wright, M. Grady, C. Pillinger, The evolution of atmospheric CO2 on Mars: The perspective from carbon isotope measurements. *J. Geophys. Res. Solid Earth* **95**, 14789–14794 (1990).
36. J. C. Aponte, H. K. Woodward, N. M. Abreu, J. E. Elsila, J. P. Dworkin, Molecular distribution, 13C-isotope, and enantiomeric compositions of carbonaceous chondrite monocarboxylic acids. *Meteorit. Planet. Sci.* **54**, 415–430 (2019).
37. C. H. House *et al.*, Depleted carbon isotope compositions observed at Gale crater, Mars. *Proc. Natl. Acad. Sci.* **119**, e2115651119 (2022).
38. K. Mimura, F. Okumura, N. Harada, Constraints on the thermal history of the Allende (CV3) meteorite by gradual and stepwise pyrolyses of insoluble organic matter. *Geochem. J.* **54**, 255–265 (2020).
39. M. Sephton *et al.*, High molecular weight organic matter in Martian meteorites. *Planet. Space Sci.* **50**, 711–716 (2002).
40. G. J. Flynn, "The delivery of organic matter from asteroids and comets to the early surface of Mars" in *Worlds in Interaction: Small Bodies and Planets of the Solar System*, H. Rickman, M. J. Valtonen, Eds. (Springer, 1996), pp. 469–474.
41. A. C. Schuerger, J. E. Moores, C. A. Clausen, N. G. Barlow, D. T. Britt, Methane from UV-irradiated carbonaceous chondrites under simulated Martian conditions. *J. Geophys. Res. Planets* **117**, 1–19 (2012).
42. H. Steininger, F. Goesmann, W. Goetz, Influence of magnesium perchlorate on the pyrolysis of organic compounds in Mars analogue soils. *Planet. Space Sci.* **71**, 9–17 (2012).
43. J. D. Carrillo-Sánchez *et al.*, Cosmic dust fluxes in the atmospheres of Earth, Mars, and Venus. *Icarus* **335**, 113395 (2020).
44. J. Oró, G. Holzer, The photolytic degradation and oxidation of organic compounds under simulated Martian conditions. *J. Mol. Evol.* **14**, 153–160 (1979).
45. A. Pavlov, G. Vasilyev, V. Ostryakov, A. Pavlov, P. Mahaffy, Degradation of the organic molecules in the shallow subsurface of Mars due to irradiation by cosmic rays. *Geophys. Res. Lett.* **39**, 13 (2012).
46. C. R. Stoker, M. A. Bullock, Organic degradation under simulated Martian conditions. *J. Geophys. Res.* **102** (E5), 10881–10888 (1997).
47. K. A. Farley *et al.*; MSL Science Team, In situ radiometric and exposure age dating of the Martian surface. *Science* **343**, 1247166 (2014).
48. C. B. Agee *et al.*, Unique meteorite from early Amazonian Mars: Water-rich basaltic breccia Northwest Africa 7034. *Science* **339**, 780–785 (2013).
49. H. B. Franz *et al.*, Large sulfur isotope fractionations in Martian sediments at Gale crater. *Nat. Geosci.* **10**, 658 (2017).
50. P. Niles, L. Leshin, Y. Guan, Microscale carbon isotope variability in ALH84001 carbonates and a discussion of possible formation environments. *Geochim. Cosmochim. Acta* **69**, 2931–2944 (2005).